MOBILE LIDAR MAPPING FOR URBAN DATA CAPTURE

Norbert Haala[a], Michael Peter[a], Alessandro Cefalu[a], Jens Kremer[b],

[a]Institute for Photogrammetry (ifp), Universitaet Stuttgart, Germany
Geschwister-Scholl-Straße 24D, D-70174 Stuttgart
Forename.Lastname@ifp.uni-stuttgart.de
[b]Ingenieur-Gesellschaft für Interfaces (IGI)
Langenauer Str. 46, D-57223 Kreuztal, Germany
J.Kremer@igi-systems.com

KEY WORDS: Three-dimensional, Point Cloud, Urban, LIDAR, Façade Interpretation

ABSTRACT:

Terrestrial laser scanning is meanwhile frequently used to capture high quality 3D models of cultural heritage sites and historical buildings. However, the collection of dense point clouds can become very labor expensive, especially if larger areas like complete historic sections of a town have to be captured from multiple viewpoints. Such scenarios opt for vehicle based mobile mapping systems which allow for so-called kinematic terrestrial laser scanning. Within the paper the performance of this approach will be described on example of the "StreetMapper" system. There 3D data collection is realized by a combination of four 2D-laser scanners, which are mounted on a vehicle based, while a high performance GNSS/inertial navigation system provides the required georeferencing information. Within our investigations the accuracy of the measured 3D point cloud is determined based on reference values from an existing 3D city model. As it will be demonstrated, the achievable accuracy levels is better than 30mm in good GPS conditions and thus makes the system practical for many applications in urban mapping.

1. INTRODUCTION

Terrestrial laser scanning (TLS) is frequently used to provide high quality 3D models of cultural heritage sites and historical buildings. Based on the run-time of reflected light pulses, these sensor systems allow for the fast, reliable and area covering measurement of millions of 3D points. However, data collection from multiple viewpoints, which is usually required for the complete coverage of spatially complex urban environments, can result in a considerable effort. Thus, 3D data capturing by so-called static TLS is usually restricted to smaller areas, which can be covered by a limited number of viewpoints. However, cultural heritage applications, which are aiming at architectural documentation can require data collection for complete places or historic parts of a town. In such scenarios, dynamic TLS from a moving platform is advantageous. Such mobile mapping systems integrate terrestrial laser scanners with a suitable system for direct georeferencing. By these means a rapid and cost effective capturing of dense 3D point clouds even for larger areas is feasible.

Within this paper, the performance and accuracy of the mobile mapping system "StreetMapper" will be discussed. Originally, this first commercially available fully integrated vehicle based laser scanning system was developed for measurement and recording of highway assets (Kremer & Hunter 2007). The StreetMapper features four 2D laser scanners integrated with a high performance GNSS/inertial navigation system. As it will be demonstrated, this configuration allows an efficient collection of dense and area covering 3D point clouds also in urban environments. Since we are aiming at the collection of architectural heritage, the main interest of our investigations is the evaluation of data quality for points measured at building facades. For this purpose vertical building faces are used as references surfaces, which are extracted from an existing 3D city model.

After a brief description of the components and the theoretical accuracy potential of the StreetMapper system in the following section, the collection of the test data is discussed in section 3. Section 4 covers the presentation and interpretation of our accuracy investigations. The final section will then conclude with a discussion and demonstrate the applicability of such data sets for the aspired collection of façade geometry.

2. STREETMAPPER SYSTEM

The StreetMapper mobile laser scanning system collects 3D point clouds at a full 360° field of view by operating four 2D-laser scanners simultaneously. The configuration of the system with the additional GPS/inertial components for positioning and orientation of the sensor platform is depicted schematically in Figure 1.

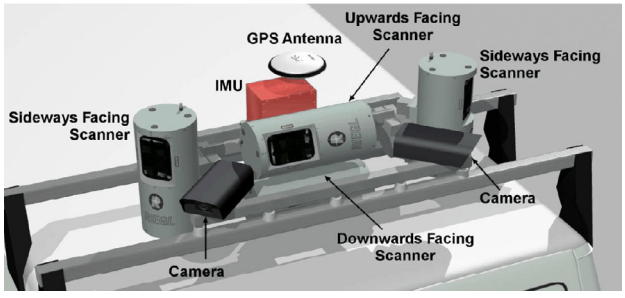

Figure 1 : Configuration of the Streetmapper system.

The required direct georeferencing during 3D point cloud collection is realized by integration of observations from GNSS (Global Navigation Satellite Systems) and Inertial Measurement Units (IMU). For this purpose the TERRAcontrol system from IGI, Germany is used. In the standard configuration the StreetMapper uses the NovAtel OEMV-3 card from NovAtel Inc, Calgary, Canada for GPS and GLONASS measurements.

However, for the project described within this paper, only GPS was operated. Since the system is optimized for data processing in the post processing mode, the real time correction, which would be available from OmniStar HP are not used.

For position and attitude determination the TERRAcontrol GNSS/IMU system is using the IGI IMU-IId (256Hz) fiber optic gyro based IMU. This Inertial Measurement Unit is successfully operated with a large number of airborne LIDAR systems and aerial cameras. Nominally, the angular accuracy of the system is below 0.004° for the roll and pitch angle. This accuracy cannot be fully exploited for the short scanning distances in this application. However, the high accuracy strongly supports the position accuracy in areas of weak or missing signal of the Global Navigation Satellite System. To gain a better aiding of the inertial navigation system during periods of poor GNSS, the GNSS/IMU navigation system for the StreetMapper is extended by an additional speed sensor. Among other benefits in the processing of the navigation data, the speed sensor slows down the error growth in periods of missing GNSS, like in tunnels or under tree cover.

In our test configuration image collection was realized by a normal consumer video camera. While this is sufficient to enable a better visual interpretation of the collected point clouds, higher demands on imaging quality can be fulfilled by operating a digital still video camera, which can be optionally mounted together with the sensors on the rigid platform.

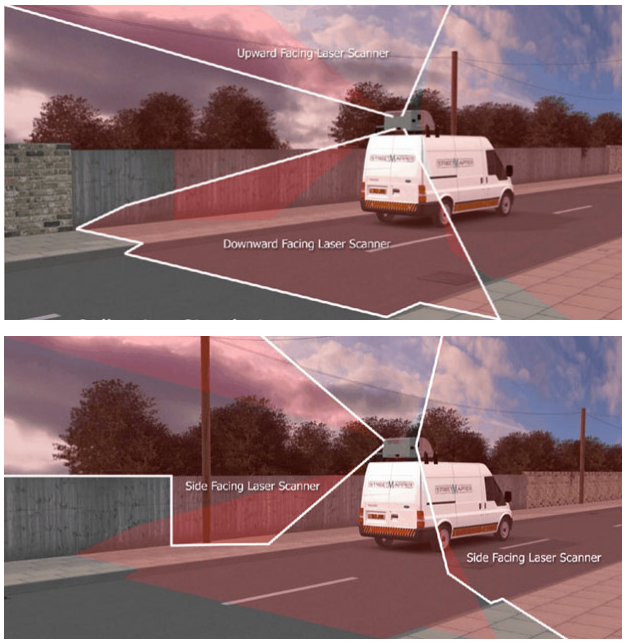

Figure 2: Field of view of the single laser scanners

The field of view available from the combination of the four different laser scanners is depicted in Figure 2. The mounting position and angles of the scanners aim to provide maximum coverage with some overlapping data between each adjacent scanner for calibration purposes. All scanners were manufactured by Riegl Laser Measurement Systems, Horn, Austria. In our test configuration, two Q120i profilers provide the upward and downward looking view at a mounting angle of 20° from the horizontal, respectively. Nominally, the Q120i has maximum range of 150 m at an accuracy of 20 mm. The side facing view to the left (with respect to the driving direction) is generated by a Q140 instrument. The respective scans to the right are measured by a Q120. The mounting angle for both of the side facing instruments is 45°. All four scanners were operated at a maximum scan angle of 80°.

3. TEST CONFIGURATION

In order to investigate the georeferencing accuracy of a mobile mapping system like StreetMapper, area covering reference measurement are required. As an example (Barber et al 2008) used approximately 300 reference coordinates, which were measured by Real Time Kinematic GPS at corner points of white road markings. During their investigations of the StreetMapper system, these points were then identified in the scanner data due to the amplitude of the reflected pulses. Alternatively to the measurement of such singular points, which can be provided at relatively high accuracies, 3D point clouds can be measured by static TLS using standard instruments and used as reference. However, this is only feasible for selected areas due considerable effort for data collection. For this reason, our investigations are based on area covering reference surfaces which are provided from an existing 3D city model for the city of Stuttgart.

This 3D city model is maintained by the City Surveying Office of Stuttgart (Bauer & Mohl, H. 2005). The roof geometry of the respective buildings was modeled based on photogrammetric stereo measurement, while the walls trace back to given building footprints. These outlines were originally collected by terrestrial surveying for applications in a map scale of 1:500. Thus, the horizontal position accuracy of façade segments are at the centimeter level since were generated by extrusion of this ground plan. Despite the fact that the façade geometry is limited to planar polygons, they can very well be used for our purposes.

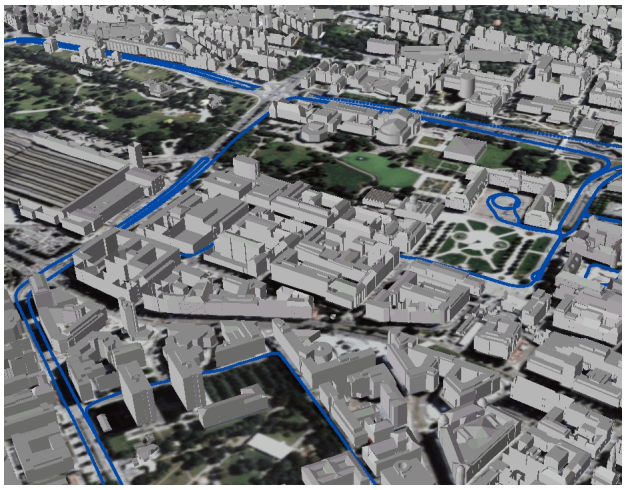

Figure 3: 3D city model used as reference data with overlaid trajectory

Figure 3 shows a 3D visualisation of the 3D city model used for the following tests. Additionally, a part of the measured trajectory is overlaid. This trajectory was captured during our test of the StreetMapper system within an area in the city centre of Stuttgart at a size of 1.5 km x 2km. During our test a distance of 13 km was covered in about 35 minutes. The measurement of the respective point clouds was realized at a point spacing of approximately 4cm.

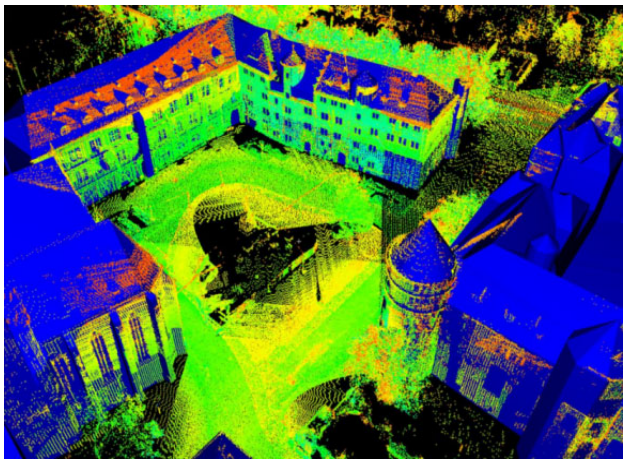

Figure 4 : Point cloud from StreetMapper aligned with available 3D city model.

Figure 4 exemplarily depicts a part of the StreetMapper point cloud at the historic Schillerplatz in the pedestrian area of Stuttgart. The measured points are overlaid to the corresponding 3D building models in order to show the quality and amount of detail of the available data.

4. ACCURACY INVESTIGATIONS

In order to assess the precision of the system, first the internal accuracy of GNSS/IMU processing as provided by the implemented Kalman filter is presented in section 4.1. Section 4.2 discusses the preprocessing of the point clouds within our evaluation scenario, while section 4.3 describes the use of the available 3D building models to determine the accuracy of the collected point clouds with respect to these reference surfaces.

4.1 Georeferencing accuracy

Like in airborne LIDAR, the accuracy of dynamic terrestrial LIDAR mapping from a mobile platform mainly depends on the exact determination of the position and orientation of the laser scanner during data acquisition. However, the GNSS conditions in a land vehicle are deteriorated by multipath effects and by shading of the signals caused by trees and buildings. Compared to an aircraft these different conditions in a land vehicle lead to different requirements for the used GNSS/IMU system.

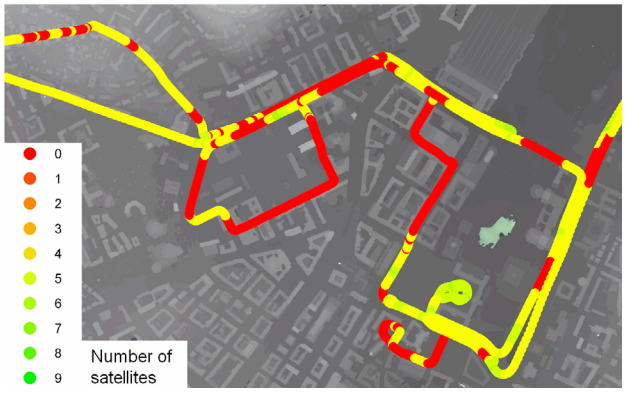

Figure 5 : Measured trajectory with number of visible satellites, overlaid to DSM of test area.

Problems due to GNSS shading are clearly visible in Figure 5 which depicts the visible number of satellites during our test. In addition to the colour coded trajectory, a grey value representation of the respective Digital Surface Model is used as the background of the figure to give an idea of the test area's topographic situation. Rather large areas of missing GNSS especially occur at very narrow streets. These areas were mainly situated in a pedestrian area of Stuttgart, were the GNSS signal was additionally shaded by a number of trees.

Figure 6 : Estimated horizontal accuracy of the trajectory after GNSS/IMU post processing.

Figure 6 gives the horizontal positioning accuracy which could be realised by GNSS/IMU post processing using the TERRAoffice software. As it is visible, under good GNSS conditions, an accuracy of the trajectory of about 3cm could be realized. For difficult conditions, where the GPS signal is shaded over larger distances, the error increases to some decimeters. However, despite the very demanding scenario it still can be kept below 1m. For mobile mapping applications, the distance between the scanner and the measured object is typically some ten meters, compared to several hundred meters for airborne laser scanning. Therefore the contribution of the GNSS positioning error to the overall error budget is much larger than the contribution of the error from the attitude determination.

4.2 Selection of point clouds

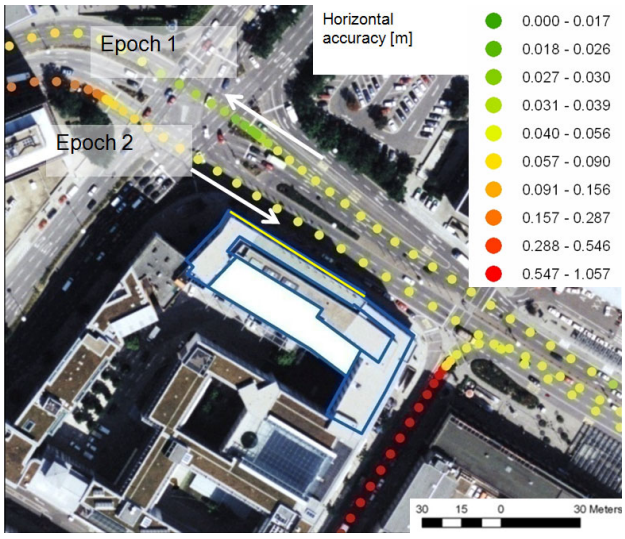

Figure 7: Ortho image with measured trajectory, selected building and part of the facade overlaid.

Figure 7 shows the ortho image for a part of our test area. In addition to the measured trajectory, the footprint of a building model, which was exemplarily selected as reference object from the available 3D city model is overlaid as a blue polygon. From this building model a façade segment is again selected, which is marked as yellow line. By these means a suitable reference

surface is available to investigate the overall error of the 3D point cloud as collected from the StreetMapper system.

Figure 7 also depicts the trajectory of the system during scanning. As it is visible, the façade was measured during 2 different epochs at two different driving directions. In epoch 1 the building was visible on the left with respect to the driving direction, while during epoch 2 the building was on the right. The georeferencing accuracy of the respective trajectory, which was provided by GNSS/IMU processing, is represented by colour coding. Since the street in front of the selected façade is relatively broad, good GPS visibility is available for that area. This resulted in an accuracy of about 3cm for the horizontal position as provided from the Kalman filter. The points, which represent the trajectory, were generated for time intervals of 1sec, clearly showing the process of slowing down and acceleration of the vehicle

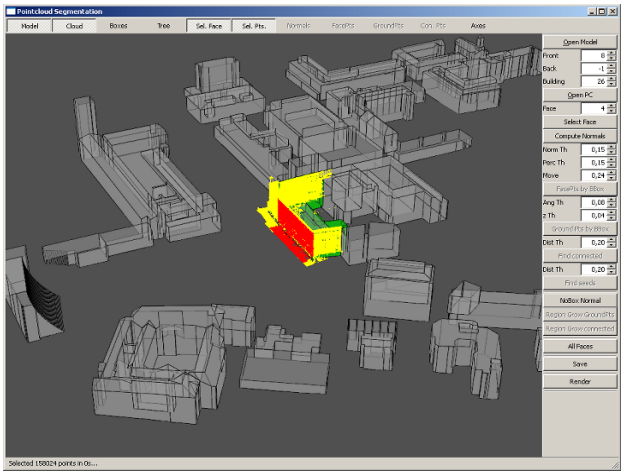

Figure 8 : 3D city model with selected reference building and corresponding section of measured 3D point cloud.

Figure 8 gives a screenshot of our GUI, which was used to select suitable reference buildings for the measured point clouds. For this purpose, the user then can interactively select single buildings and building facades from the available 3D city model. The relevant 3D point measurements are then extracted automatically by a simple buffer operation. Within Figure 8, the available LiDAR points for the building already depicted in Figure 7 are marked in yellow, while measurements corresponding to the selected façade are marked in red and the selected building is highlighted in green.

4.3 Investigation of point clouds

After the selection process, the respective façade points are transformed to a local coordinate system as defined by this façade plane. The resulting vertical distances of the measured points can then be used for a further error analysis. In order to get a first impression of the measurement accuracy, Figure 9 shows the vertical distances of the LiDAR measurements represented as colour coded points. As it is visible, points were selected from 5.8cm in front to 61.0cm behind the given façade plane. Most of the points behind the plane refer to measurements at window surfaces.

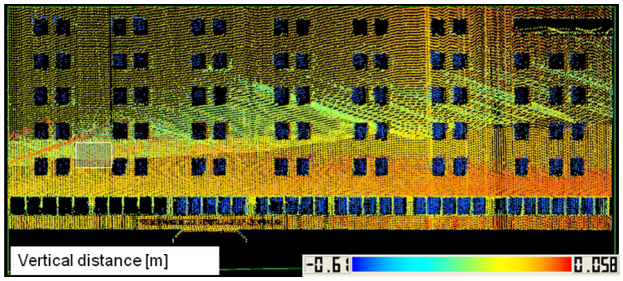

Figure 9 : Color-coded vertical distances of the measured 3D point cloud with respect to the corresponding façade surface.

For further analysis, the measured LiDAR points were used to estimate planar surface patches by least squares adjustment, which then were compared to the given façade polygon from the city model. In this way, the points within the white polygon of Figure 9 resulted in a shift between the estimated and the reference plane of -13.8cm. The horizontal accuracy of the given building façade is in the order of several centimeters. Thus, this shift can in principle result both from errors in the LiDAR measurement and the reference model. For this reason further investigation were carried out using additional features of the collected 3D points like the measured range, the look angle both with respect to the sensor platform and the reference façade, the respective scanner and the time of measurement. This is feasible since the StreetMapper provides the 3D point cloud in the ASPRS LAS format (Graham 2005).

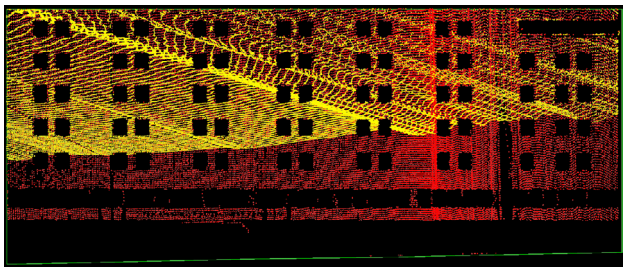

Figure 10: Points measured during epoch 1 from upward and left looking scanner, represented by yellow and red points, respectively.

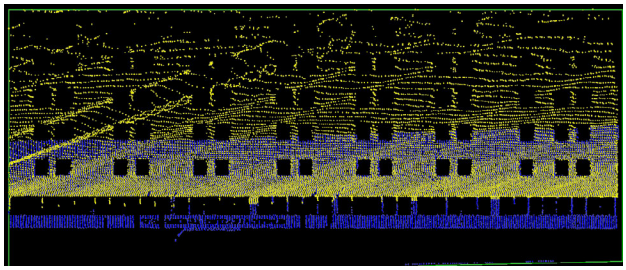

Figure 11: Points measured during epoch 2 from upward and right looking scanner, represented by yellow and blue points, respectively.

For our investigations, the separation of the measured point cloud with respect to the different scanners and measurement epoch was of special interest. As already discussed, the façade was measured during 2 different epochs. Figure 10 shows the points measured during the first pass of the vehicle (epoch 1). In this epoch measurements from the left and the upward looking scanner are available, which are represented by the red and yellow points, respectively. During these measurements, the perpendicular distance between the vehicle and the building façade was approximately 25m, resulting in a mean value of the measured ranges of about 41m. Figure 11 depicts the

measurements during the second pass of the vehicle, when the building was on the right side with respect to the driving direction. Thus, points from the right scanner looking scanner, (blue), are available together with points from the upward looking scanner (yellow). Due to the shorter distance between vehicle and the building, only the lower part of the façade was captured from the side looking scanner in the second epoch. Planar patches were then estimated and compared to the façade surface for the respective scanners and epochs. The results of these investigations are summarized in Table 1.

Scanner	Epoch	Shift [cm]
l+r+u	1+2	-13.8
l	1	-13.5
r	2	-12.6
u	1+2	-15.4
u	1	-25.7
u	2	-0.08

Table 1: Estimated planes for the selected patch, separated for different scanners and measurement epochs.

The determined shift values within Table 1 again refer to points within the white polygon already depicted in Figure 9. The first line of Table 1 shows the result for the combination of point measurements from all scanners (left, right, up, l+r+u) at all epochs (1+2). As already discussed in section 4.2, the shift of -13.8cm between the measured plane and the reference façade is in the order of the available quality of the building model.

For perfect georeferencing and system calibration, no differences between the measurements from different scanners at different epochs should be visible. However, the colour coded vertical distances for all available points already depicted in Figure 9, apparently show some systematic effects. These effects are verified by the further values in Table 1. The second row gives the shift for an adjusted plane using the points from the left looking scanner (l) captured during period 1 (red points in Figure 10). This resulted in a distance of -13.5cm with respect to the given façade. These measurements fit very well to the shift of the points measured from the right looking scanner (r) in period 2 (blue points in Figure 11), which resulted in a distance of -12.6cm. However, if data from the upward looking scanner (u) (yellow points in Figure 10 and Figure 11, respectively) is examined for periods 1 and 2, the shift is -15.4cm. If these points are further separated with respect to the different epochs (rows 5 and 6) the shift is -25.7cm for epoch 1 and -0.08cm for epoch 2.

As it is visible in rows 2 and 3 of Table 1, the measurements from the left and right looking scanner , which were captured at different epochs result in a difference between the estimated planar patches of just 0.9cm. This fit indicates a quite good georeferencing accuracy for both epochs and a good calibration of both scanners. Apparently, the differences of the estimated planes to the reference plane apparently result from the error in the given 3D building model. In contrast, the estimated planar patches from the measurements of the upward looking scanner show considerable differences between epoch 1 and 2. The opposite signs of the deviations apparently trace back to the different driving directions during point measurement. Thus, the deviation can be explained by an improper boresight calibration of the upward looking scanner. This effect could be verified for other building facades of our test data set.

In general, such calibration problems, which are well known from the processing of airborne LiDAR and can be solved by suitable post processing. In our test, the boresight calibration was refined for the upward scanner, which resulted in a change of that scanner orientation (heading) with respect to IMU of 0.1°.

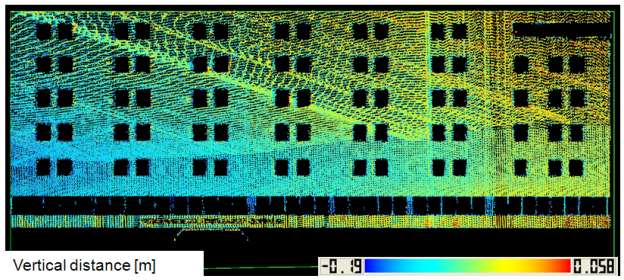

Figure 12 Color-coded vertical distances after refined calibration.

After the refined calibration the georeferenced 3D point cloud was again used to compute vertical distances with respect to the corresponding façade surface. The result is depicted in Figure 12. In contrast to Figure 9, systematic effects of the color-coded vertical distances are no longer visible.

Scanner	Epoch	Shift [cm]	Std.dev. [cm]
l+r+u	1+2	-7.8	4.7
l+u	1	-7.4	4.6
u+r	2	-9.0	4.1

Table 2 : Estimated planes for the completed building façade

This improvement is also verified by the results in Table 2. The shift and RMS values in Table 2 were determined from all LiDAR points for the complete building façade, which had a size of 26m x 60m. As it is visible, the values fit very well for the different epochs and scanners. Apparently, remaining deviations of the measured points can be explained by the limited accuracy of façade from the 3D building model.

4.4 Shaded GPS conditions

As it is already visible in Figure 5 and Figure 6, for some areas the shading of the GNSS satellites results in a georeferencing error up to 1m for the horizontal position. Despite the limited quality of the absolute position in the mapping coordinate system, such 3D point measurements during bad GPS conditions are still useful, especially if mainly their relative position is exploited.

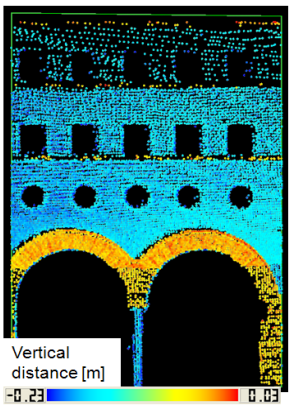

Figure 13: Captured point cloud during shaded GPS conditions.

For the example given in Figure 13, rather large differences between the reference building and the estimated plane occurred to long term GPS shading in that area. However, the standard deviation of the estimated planes is 5cm if points from the left and upward looking scanner are combined and 2.6cm if the points are separated for each scanner. For this reason, the

collected point cloud can still be used for applications like precise distance measurements or the extraction of features of interest like windows or passages, if a certain error for their absolute position is acceptable.

5. CONCLUSIONS AND OUTLOOK

Within our study, the feasibility of the StreetMapper system to produce dense and accurate 3D measurements has been demonstrated. Such densely sampled 3D points at urban areas can for example be used very well to geometrically reconstruct fine geometric details of building facades like windows, balconies, stonework and ornaments. Within our work, the required interpretation of terrestrial LiDAR point clouds is supported efficiently by the use of a coarse building model that describes the overall geometry of the building in a polyhedral approximation (Becker & Haala 2007). As already discussed in section 3 such coarse representations are frequently available from existing 3D city models, which are usually generated from airborne data collection.

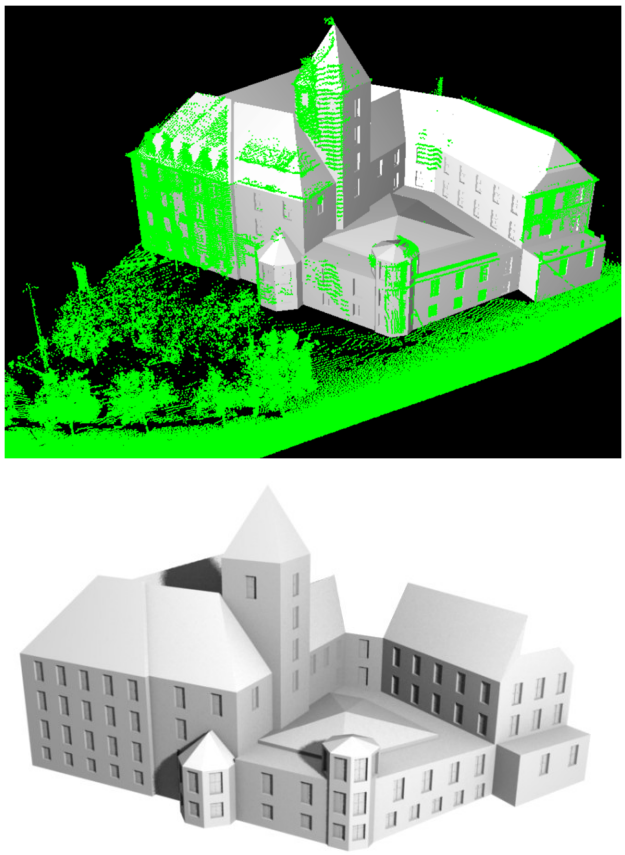

Figure 14 : Facade reconstruction for the “Lindenmuseum” with and without measured 3D points overlaid.

Figure 14 depicts an example of our ongoing work, where the planar facades of the existing 3D city model of Stuttgart is refined using the collected StreetMapper point clouds. As it is visible, geometric façade structure like windows and doors are automatically generated for the respective coarse 3D building model. Existing 3D city models can also be used to improve the absolute accuracy of the georeferencing process of the 3D point cloud collection. This can for example be necessary for areas of shaded GPS conditions. For this purpose the measured 3D point cloud can be registered to the given 3D building model by an iterative closest point (ICP) algorithm as presented in (Böhm & Haala 2005).

6. REFERENCES

Barber, D., Mills, J. & Smith-Voysey, S. [2008]. Geometric validation of a ground-based mobile laser scanning system . *ISPRS Journal of Photogrammetry and Remote Sensing* **63**(1, January 2008), pp.128-141 .

Bauer, W. & Mohl, H. [2005]. Das 3D-Stadtmodell der Landeshauptstadt Stuttgart. In: Coors V. & Zipf A.e. (eds.), *3D-Geoinformationssysteme: Grundlagen und Anwendungen* Wichmann Verlag.

Becker, S. & Haala, N. [2007]. Combined Feature Extraction for Façade Reconstruction. Proceedings Workshop on Laser Scanning - LS2007 .

Böhm, J. & Haala, N. [2005]. Efficient Integration of Aerial and Terrestrial Laser Data for Virtual City Modeling Using LASERMAPS. IAPRS Vol. 36 Part 3/W19 ISPRS Workshop Laser scanning 2005 , pp.192-197.

Graham, L. [2005]. The LAS 1.1 standard. *Photogrammetric Engineering and Remote Sensing* **77**(7), pp.777-780.

Kremer, J & Hunter, G. [2007]. Performance of the StreetMapper Mobile LIDAR Mapping System in “Real World” Projects . Photogrammetric Week '07, pp. 215-225.